This is an accepted pre-print version for the European Control Conference 2021

Enhanced LMI-based Damping Control in Power Networks through a High Voltage Direct Current Line

Sjoerd Boersma[1], Luigi Vanfretti[2] and Abdelkrim Benchaib[3]

***Abstract*— Large interconnected power networks are arguably some of the most complicated man-made systems to understand and characterize. This becomes even more complicated due to the surge of renewables that are connected (possible via HVDC lines) to the network. Faults, such as the tripping of an electricity line, can easily occur in a network, which can cause undesired oscillatory behaviour. This paper proposes an output-feedback controller that aims at diminishing these oscillations. The presented controller consists of a state-feedback gain and a Kalman filter and is tuned by employing an in this work identified model. The proposed controller ensures a lower bound on the closed-loop damping coefficients of the network.**

I. INTRODUCTION

An electrical power system is a large-scale inter-connected system (power network) that consists of generators, loads, conductors, protective devices, power electronics and other electrical components. An example of such a power network is the electricity grid that generates, consumes and transports electrical power from generators (such as a wind farm [1]) to consumers. This transport of bulk power can go through conventional Alternating Current (AC) lines or High Voltage Direct Current (HVDC) lines whereas the latter increases in popularity due to the advantages it has regarding the transport of large quantities of power over relatively long distances. For example, a wind farm can be placed very far in the sea, while its produced power is transported to the grid through an HVDC line [2]. Traditionally HVDC links are used to interface two asynchronous power systems, either with different frequencies (e.g. 50 Hz to 60 Hz, in Japan) or the same synchronous frequency but operated separately (e.g. as in the USA). A less common approach is to have an embedded HVDC link that interfaces two major areas of a synchronous grid, as in the case of the US Pacific DC link [2], which is gaining recent attention because of the need to increase power transfer capabilities between specific areas. In particular, in the Continental European power grid, the French and Spanish networks have been recently coupled through an HVDC link, connecting the Baixas (France) and Santa Llogaia (Spain) substations [3].

A phase angle difference between areas gives a measure of the power flow through the connecting AC lines form one to the other area, the larger the phase angle difference, the larger the power transfer between those areas. As other systems, a power network can also be characterized by a number of modes. From these, there are only a couple of dominant ones. These are local, which are found within each area itself or inter-area modes, which are the modes between different areas. When measurements are available, system identification methods can be used to find these dominant ones such that the derived model can be used for monitoring [4] and control design. In general, the most dominant modes are the inter-area ones and, when low-damped, can cause undesired oscillatory behavior leading to a system blackout [5]. For example, when a major power line in the network trips, a low damped inter-area mode is excited and undesired oscillatory behavior is observed in the measurements. Controllers that aim to damp these oscillations are referred to as damping controllers. Conventional damping controllers are deployed in synchronous generators and are known as Power System Stabilizers (PSS), while Flexible Alternating Current Transmission Systems (FACTS) can include a supplementary damping controller [6]. Another way to damp these oscillations is the utilization of an HVDC line that is embedded in the network [7]. Consequently, the HVDC line is not only used for the transport of bulk power, but also employed to provide other services like damping control. The main idea is that when oscillations are measured, the HVDC line counteracts these oscillations modulating the active power flow that is transported [8]. This type of damping control can be employed together with the usage of standard techniques based on PSS and FACTS supplementary controls. However, the world-wide installation of HVDC damping control schemes is rather limited due to different design and operational challenges.

In [9], the authors propose a damping controller using an iterative LQR design method such that desired closed-loop pole locations are obtained assuming full state knowledge. The employed model for control design is obtained via first principle modeling, which is challenging for real-world large-scale grids. In [10], the authors propose a complete control solution to the power network's damping problem. Subspace Identification is used to identify a model and it is used to design a Luenberger observer and state-feedback controller. The user has to specify desired closed-loop poles in order to obtain the controller. In [11], the authors propose a LQG (Kalman filter and LQR) damping controller. Standard PSS are used to damp the local modes and the proposed LQG

*This work is supported by SuperGrid-Institute

[1]Sjoerd Boersma is with the Wageningen University, Wageningen, Holland sjoerd.boersma@wur.nl

[2]Luigi Vanfretti is with the Department of Electrical, Computer, and Systems Engineering, Rensselaer Polytechnic Institute, Troy, USA

[3]Abdelkrim Benchaib is with SuperGrid-Institute, Lyon, France

controller is used to damp the inter-area modes. The utilized controller design model is based on a linearized Simulink (reduced order) model, which is a bold assumption. The proposed framework does not entail system identification, which is necessary for control design of these type of systems [8]. More recent work on damping control via an HVDC line is found in [12], where a damping controller is proposed that contains a PI-controller and therein called feed-forward term. The presented controller shows promising results although it is not reported how the controller gains are determined.

Because the operational experience with HVDC links for damping control is limited, it not obvious for the majority of Transmission System Operators (TSOs) what the desired closed-loop pole locations are, specially since large-scale models are difficult to maintain. In addition, tuning of weighting matrices for control design is challenging in a domain where most controls are designed with classical control methods, e.g. root-locus [13]. Hence, for practical purposes, it can be most beneficial to define a lower bound on the network's closed-loop mode damping and speed, and successively find a controller to mitigate them. In addition, it is necessary that the controller design model is updated following time-varying network's dynamics. With the controller framework proposed in this work, both these criteria are satisfied. More precisely, this paper proposes an output-feedback damping controller that regulates the active power through the HVDC line such that oscillatory behavior is diminished. The output feedback controller contains a state-feedback gain and a Kalman observer. The former is evaluated after solving an optimization problem containing Linear Matrix Inequalities (LMIs), which is different from the LQR design method proposed in previous works. Via these LMIs, an user-defined upper bound on the closed-loop damping coefficient and the state's speed of convergence are imposed through control [14], [15]. The Kalman observer demands for a model that is also identified, this is achieved in this work by employing the Prediction Error Method (PEM) [16], [17]. The proposed identification method is executed when desired such that an updated controller design model is evaluated. The main contributions of this work to the power system damping problem are:

1) A full control design solution is given that includes system identification, control and observer design.
2) The application of an LMI-based controller with user-defined upper bound on the closed-loop damping coefficient as tuning parameter.

The employed software are MATLAB (for system identification and control design) and the Modelica tool Dymola in combination with the OpenIPSL library [18] (for nonlinear power system modeling and simulation). The library was built to model nonlinear power system networks using the phasor (*i.e.*, positive-sequence) modeling approach.

This paper is organized as follows. Section II discusses the nonlinear test network that is considered in this work. Then in Section III, a linear model is identified and then is used for control design, as discussed in Section IV. Finally, Section V presents the simulation results and this paper is concluded in Section VI.

II. TEST NETWORK

The test network used in this work is the 4-machine 2-area Kelin-Rogers-Kundur power system model [19] (hereinafter Kundur network) with an embedded HVDC line. The latter is connecting the two areas as is illustrated in Fig. 1. Here it is shown that the network consists of 4 generators (G_i), 4 transformers, 11 buses and one HVDC line (turquoise). This nonlinear network is simulated in the Modelica tool Dymola and assembled using the OpenIPSL library [18] and contains 45 state variables.

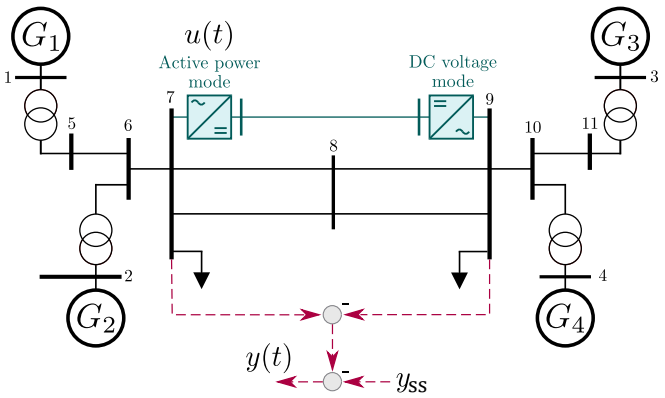

Fig. 1. Schematic representation of the Kundur network that includes an HVDC line with $y(t) = \delta\varphi(t)$ the phase angle difference measured relatively to a steady-state value y_{ss} and $u(t) = P_{hvdc}(t)$ the active power through the HVDC line measured relatively to a steady-state value u_{ss}.

The network is characterized by the following nonlinear model:

$$\dot{x}(t) = f(x(t), u(t)), \quad y(t) = h(x(t), u(t), v(t)) \tag{1}$$

with time t, measurement $y(t) = \delta\varphi(t) \in \mathbb{R}$ the phase angle difference between the two areas measured relatively to a steady-state value y_{ss}, control signal $u(t) = P_{hvdc}(t) \in \mathbb{R}$, which is the active power through the HVDC line measured relatively to a steady-state value u_{ss}, measurement noise $v(t)$) with standard deviation $\sigma_v = 10^{-3}$, state variable of the nonlinear network $x(t)$ and unknown nonlinear mappings $f(\bullet), h(\bullet)$. In the following section, a linear (low-order) model is identified that describes the dominant characteristics of the network.

III. SYSTEM IDENTIFICATION

The system identification technique referred to as the Prediction Error Method (PEM) [16], [17] is employed to identify a linear model. The Output Error model structure is assumed and defined as:

$$\hat{y}_k = H(z, \theta)u_k + e_k, \tag{2}$$

with k the discrete-time, $z \in \mathbb{C}$, θ the unknown parameter vector and linear model $H(z, \theta)$. Furthermore, $\hat{y}_k \in \mathbb{R}$ is the identified model's output that estimates the measured output

$y(t)$, u_k the control signal and $e_k \in \mathbb{R}$ represents Gaussian distributed noise with standard deviation σ_e and zero mean. The structure of $H(z,\theta)$ is defined as:

$$H(z,\theta) = \frac{\theta_{n_a+1} z^{n_b-1} + \cdots + \theta_{n_a+n_b}}{z^{n_a} + \theta_1 z^{n_a-1} + \cdots + \theta_{n_a}} \cdot z^{-n_k}, \quad (3)$$

with $\theta = \begin{pmatrix} \theta_1 & \theta_2 & \dots & \theta_{n_a+n_b} \end{pmatrix}$. The parameters to be determined in the identification procedure are n_a, n_b, n_k. For the PEM, an experiment for system identification needs to be conducted on the network in order to obtain information (the measurement). This is done via perturbing the network with an excitation signal during the experiment, which is an acceptable assumption considering past and recent practices [20]. In this work, the network is excited with a multi-sine signal, *i.e.*,

$$u_k = \sum_{r=1}^{M} A_r \sin(\omega_r k + \varphi_r). \quad (4)$$

Here, $A_r, \varphi_r, \omega_r, M$ are the user-defined magnitude, phase and frequency of the r^{th} sinusoidal component, respectively, and M the number of frequency components in the multi-sine signal. In [4], the amplitudes A_r are optimized to ensure an upper bound on the damping estimation's variance. In this work, A_r is found empirically such that a validated model is obtained and φ_r is chosen randomly. Furthermore, ω_r is defined as a grid containing the frequency components of interest. These are the target frequencies around where the identified model will be more accurately estimated than the frequency components outside of this grid. Clearly, ω_r should contain the frequency components of the closed-loop system since it is here important that the identified model is the most accurate. Note that the experiment for system identification can easily be re-performed such that an updated controller design model is obtained. This is important since network dynamics are changing over time and the controller needs to be updated accordingly.

The identified model $H(z,\theta)$ has, after neglecting the pure delays, the following continuous-time minimal (observable and controllable) state-space realization:

$$\dot{\hat{x}}(t) = A\hat{x}(t) + Bu(t), \qquad \hat{y}(t) = C\hat{x}(t) + Du(t), \quad (5)$$

with $A \in \mathbb{R}^{n_a \times n_a}, B \in \mathbb{R}^{n_a \times 1}, C \in \mathbb{R}^{1 \times n_a}$ and $D \in \mathbb{R}$. The state-space matrices A, B, C, D are used for control and observer design. Since the identified model has $D = 0$, it is not further considered in the formulas presented in this work.

SYSTEM IDENTIFICATION RESULTS

One experiment for system identification is performed. After re-sampling the measurement y_k and excitation signal u_k to a sample period of h, N data points are left in the data. Indeed, h, N are seen as tuning parameters and depend on the size of the network and on the dynamics that need to be described by the identified model. A large N results in a more accurate identified model, however a larger experiment length is in practice not always desirable. Increasing the sample period h, will remove higher frequencies from the data and, consequently, can not be identified anymore. The tuning parameters $A_r, \omega_r, n_a, n_b, n_k$ are found such that a validated identified model is obtained. This validation is ensured by imposing a 1-standard deviation value requirement, which gives 68.27% confidence region, so that each parameter is below the 5% with respect to the estimated value. The 1-standard deviation value for each parameter is evaluated using the MATLAB function `present.m` and the final found user-defined parameters for system identification are shown in Table I.

TABLE I

SYSTEM IDENTIFICATION TUNING PARAMETERS.

Parameter	A_r	ω_r (Hz)	n_a	n_b	n_k	h (s)	N
Value	1	$[0.1, 5]$	3	3	3	0.05	1200

Figure 2 depicts the Bode magnitude plot of the identified continuous-time model $H(s)$ (black). This is compared to the Bode magnitude plot of the linearized nonlinear network (gray), which is obtained using [21]. As shown, the identified model approximates the linearized network around the important frequencies (0.5-1 Hz). In this band, the resonance (inter-area mode) and anti-resonance are found. On the other hand, the comparison is less accurate for frequencies above 1 Hz where the local modes are found. Consequently, the HVDC damping controller will target the damping of the inter-area mode and not the local modes. Note that the linearized model contains 45 state variables, while the identified model only contains 3 state variables. This is one of the the reasons why the identified model is suitable for control design. Also, the control results in Section V show that the identified model is sufficient for this purpose.

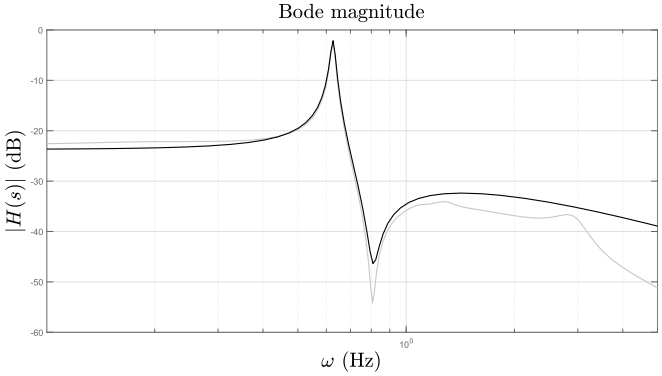

Fig. 2. A Bode magnitude plot comparison between the identified continuous-time model $H(s)$ (black) and the linearized nonlinear network (gray).

IV. CONTROL DESIGN

The proposed control design approach is presented in this section. The controller consists of a state-feedback gain (Section IV-A) and a Kalman observer (Section IV-B). Both form an output feedback controller that is defined in Section IV-C.

A. STATE-FEEDBACK GAIN

An LMI-based design technique is used to find a state-feedback gain K that is used in the control law $u(t) = -K\hat{x}(t)$. The user-defined options are a lower bound on the closed-loop damping coefficient ζ_{cl} and an upper and lower bound on the decay rate of the closed-loop states, which are $\alpha_{\max}$ and $\alpha_{\min}$, respectively. The decay rate of the states is seen as a measure of speed of the closed-loop and depends, among others, on the actuators' speed. In this case, the actuator is an HVDC link, which is relatively fast. The following optimization problem is solved to find K [14], [15]:

$$\min_{Y,X>0,\gamma>0} \quad \gamma \tag{6}$$

subject to:

$$XA^T + AX - Y^TB^T - BY < 2\alpha_{\min}X \tag{7}$$

$$XA^T + AX - Y^TB^T - BY > 2\alpha_{\max}X \tag{8}$$

$$\begin{pmatrix} \Pi_{11} & \Pi_{12} \\ \Pi_{21} & \Pi_{22} \end{pmatrix} < 0 \tag{9}$$

$$\begin{pmatrix} \gamma I_{n_a} & Y^T \\ Y & 1 \end{pmatrix} > 0 \tag{10}$$

with

$$\begin{aligned} \Pi_{11} &= \sin(\beta)\left(XA^T + AX - Y^TB^T - BY\right) \\ \Pi_{12} &= \cos(\beta)\left(-XA^T + AX + Y^TB^T - BY\right) \\ \Pi_{21} &= \cos(\beta)\left(XA^T - AX - Y^TB^T + BY\right) \\ \Pi_{22} &= \sin(\beta)\left(XA^T + AX - Y^TB^T - BY\right) \end{aligned} \tag{11}$$

and $\beta = \arccos(\zeta_{\text{cl}})$. The state-feedback gain is evaluated as:

$$K = YX^{-1}. \tag{12}$$

The LMIs (constraints) given in (7), (8) and (9) impose a bounded area in the complex plane where the closed-loop poles are placed by the gain K. This is illustrated in Fig. 3. The LMI in (10) together with the cost (6) minimize the control action. Indeed the LMI in (10) is equivalent to $||Y||_\infty < \gamma$. Since γ is minimized and K depends linearly on Y, the state-feedback gain K is minimized only through Y.

STATE-FEEDBACK GAIN DESIGN RESULTS

Table II shows the user-defined parameters that are used to design the state-feedback controller. These parameters are found such that the controller damps the oscillations without over-actuation through the HVDC line.

TABLE II
CONTROL DESIGN TUNING PARAMETERS.

Parameter	ζ_{cl}	$\alpha_{\min}$	$\alpha_{\max}$
Value	0.95	-4.5	-5

In Fig. 4, the eigenvalues of the matrix $(A - BK)$ (eig$(A - BK)$) are depicted together with the open-loop poles (eig(A)). The pole close to the imaginary axis causes the oscillatory behavior in the network, while the second makes the control response stiff. These type of poles are typical power networks. Imposing the control law $u(t) = -K\hat{x}(t)$ and finding K by solving the optimization problem presented in (6), moves the eigenvalues of the matrix $(A - BK)$ in such way that the damping and control response is improved, and thus, less oscillatory behavior is observed as shown in Section V.

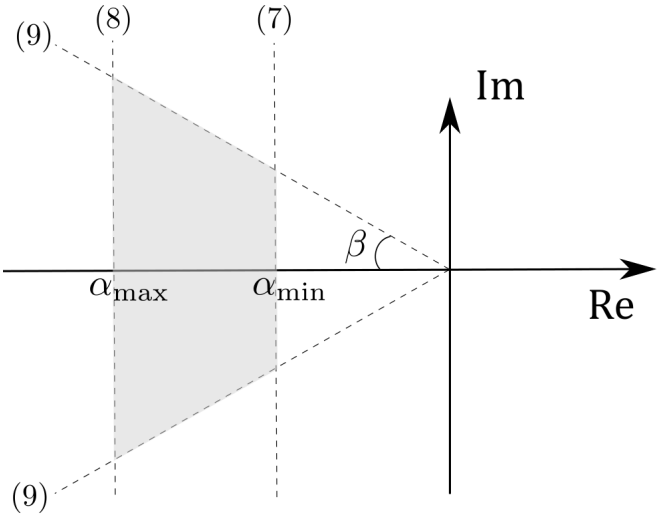

Fig. 3. Representation of the LMIs given in (7), (8) and (9) in the complex plane. The gray area indicates the bounded are where the closed-loop poles are going to be thanks to closing the loop with K. Furthermore, $\beta = \arccos(\zeta_{\text{cl}})$ with ζ_{cl} the closed-loop damping coefficient.

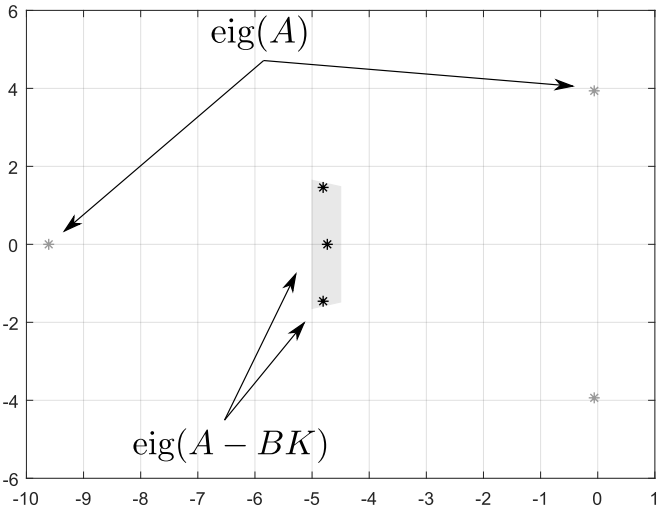

Fig. 4. Subset of the closed-loop poles (which are the eigenvalues of the matrix $(A - BK)$) and open-loop poles (which are the eigenvalues of the A matrix) depicted in the complex plane. The constrained area is shown in gray as has been done in Fig. 3.

The designed state-feedback gain's effectiveness can be appreciated even more when inspecting the Bode magnitude plots of both the open-loop case (identified model) and the closed-loop case with $u(t) = -K\hat{x}(t)$ in (5). These frequency responses are depicted in Fig. 5. Clearly, the low damped inter-area mode is diminished thanks the state-

feedback gain K. This inter-area mode is the most dominant mode and causes the most oscillatory behavior in a network as discussed previously.

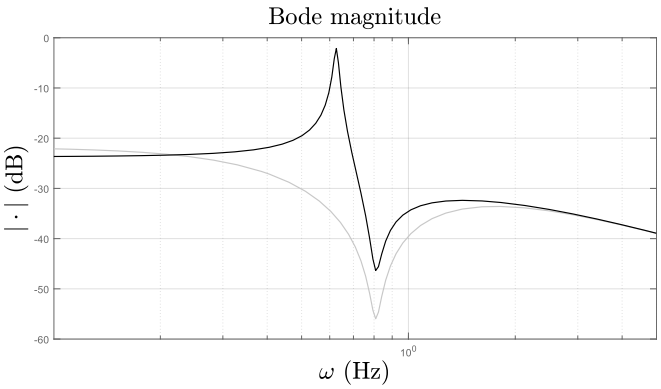

Fig. 5. The Bode magnitude plots of the identified continuous-time model $H(s)$ considered as the open-loop case (black) and the closed-loop case (gray) where $u(t) = -K\hat{x}(t)$ in (5) is substituted.

Even though an identified model is available (and thus also $\hat{x}(t)$), the initial conditions are not known. Therefore, a Kalman observer is used that is providing a $\hat{x}(t)$ that is corrected by the measurement $y(t)$.

B. KALMAN OBSERVER

In this work, a Kalman observer is designed. It takes on measurements $y(t)$ from the network and provides a state estimation $\hat{x}(t)$ that is an input to the previously defined control gain. This assumption is valid in practice, as such type of measurements can be made available by the use of Phasor Measurement Units (PMUs) [22]. The observer has the following state-space model:

$$\begin{aligned} \dot{\hat{x}}(t) &= (A - LC)\hat{x}(t) + Bu(t) + Ly(t), \\ \hat{y}(t) &= C\hat{x}(t), \end{aligned} \tag{13}$$

with L the Kalman gain that, after assuming that the state and measurement noise are not correlated, is found by evaluating:

$$L = PC^T V^{-1}, \tag{14}$$

where the steady-sate covariance matrix of the innovation sequence P satisfies the Ricatti equation

$$AP + PA^T - PC^T V^{-1} CP = W, \tag{15}$$

with the matrices W, V the steady-state covariance matrices of the assumed to be Gaussian white process and measurement noise, respectively. These are seen as tuning variables of the observer. Note that in order to derive (13) from (5), the latter is appended with the additional input $L(y(t) - \hat{y}(t))$.

KALMAN OBSERVER DESIGN RESULTS

Table III presents the tuning variables that are found for the Kalman observer. These parameters are found such that the identified model's output $\hat{y}(t)$ tracks the measurement $y(t)$ and such that eig$(A-LC)$ and eig$(A-BK)$ are located relatively closely together.

TABLE III
OBSERVER DESIGN TUNING PARAMETERS.

Parameter	V	W
Value	10^{-3}	10^{3}

Another metric to asses the performance of the observer is the comparison between $x(t)$ and $\hat{x}(t)$. However, $\hat{x}(t)$ comes from an identified model employing the PEM. Consequently, the meaning of the states is not known, *i.e.*, it can be a linear combination of speeds, phase angles and other physical parameters. It is therefore not useful to compare $x(t)$ and $\hat{x}(t)$.

C. OUTPUT-FEEDBACK CONTROLLER

Both the state-feedback gain and the Kalman observer are combined to form an output-feedback controller. This controller has the following state-space realization [23]:

$$\begin{aligned} \dot{\hat{x}}(t) &= (A - BK - LC)\hat{x}(t) + Ly(t), \\ u(t) &= -K\hat{x}(t). \end{aligned} \tag{16}$$

In order to derive (16) from (13), simply substitute $u(t) = -K\hat{x}(t)$ and take $u(t)$ as the output of the output-feedback controller. A schematic representation of the proposed control scheme is depicted in Fig. 6.

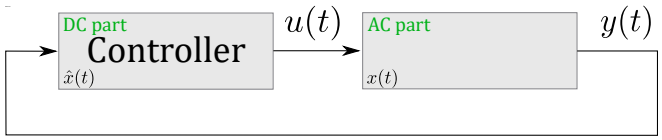

Fig. 6. A schematic representation of the proposed closed-loop control scheme. The controller is governed by the state-space model given in (16) with state $\hat{x}(t)$.

V. SIMULATION RESULTS

This section presents the open and closed-loop control simulation results. The previously designed controller (16) is implemented in the Modelica tool Dymola. The therein simulated nonlinear network is subjected to a power line trip between bus 7 and 8 (see Fig. 1), starting at $t = 5.0$ and restored at $t = 5.3$ seconds. Note that both the type and time of disturbance are unknown to the controller. As discussed in the introduction, these type of disturbances occur regularly in power networks and result in oscillatory behavior in the measurements. The proposed controller damps these oscillations such that less stress in the network, which can be seen in the phase angle difference response shown in Figure 7. The figure shows a comparison between the open-loop case and the closed-loop case. The results illustrate the controller's effectiveness since it is able to damp the oscillation significantly with respect to the open-loop case (see the first subplot). For this, the controller is injecting and withdrawing active power from the grid via the HVDC link. This is shown in the second subplot shown in Fig. 7. Observe that the control response is commensurate (and lower) that that seen in recent experimental results [8].

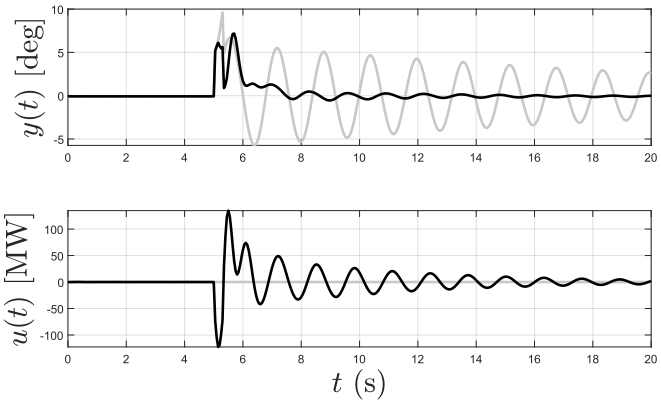

Fig. 7. Comparison between open-loop (gray) and closed-loop (black) simulation results. During the simulation, one line is tripped between $t = 5.0$ to $t = 5.3$ seconds resulting in oscillatory behavior. The proposed damping controller is able to diminish these oscillations with respect to the open-loop case.

VI. CONCLUSIONS

Electrical power networks are complex large-scale interconnected systems that transport large amounts of electricity from generation sites, e.g. wind farms, to consumption centers, e.g. metropolitan and industrial cities. The existing power transmission infrastructure is facing challenges to meet new requirements for de-carbonization, which demands to transport new renewable energy production across larger geographical areas. To achieve this goal, AC interconnections are being reinforced with HVDC lines to increase power transfer. Next to that, they can provide ancillary services if equipped with well designed control systems. An example of such services is to damp oscillations that can emerge due to a major network disruption. While current methods exist to damp these oscillations, the usage of an HVDC links to provide damping control is rather limited. This is due to many challenges, among which adequate control design is chief.

This paper proposed the utilization of an output-feedback control design method capable of damping inter-area oscillations by exploiting an HVDC line equipped with a damping control system. The control design method requires an identified model. This identification procedure was also presented in this work. The user-defined parameters for the controller design are the closed-loop damping coefficient and the rate of convergence of the closed-loop states. The controller has successfully been tested on a relatively small benchmark network model by performing non-linear simulations. It has been shown that oscillations are damped significantly with respect to the open-loop case illustrating the controller's adequate performance.

Future work is focused on testing the damping controller design method on larger networks and also on networks with multiple HVDC lines. Other subsequent work is the design of a damping controller that is not only focused on the inter-are-modes, but also aims to damp the local modes.

REFERENCES

[1] S. Boersma, B. M. Doekemeijer, P. M. O. Gebraad, P. A. Fleming, J. Annoni, A. K. Scholbrock, J. A. Frederik, and J. W. van Wingerden, "A tutorial on control-oriented modelling and control of wind farms," *American Control Conference*, 2017.

[2] S. Dennetiere, H. Saad, Y. Vernay, P. Rault, C. Martin, and B. Clerc, "Supporting energy transition in transmission systems: an operator's experience using electromagnetic transient simulation," *Power and Energy Magazine, vol. 17(3), pp. 48-60*, 2019.

[3] R. L. Cresap and Mittelstadt, "Small-signal modulation of the Pacific HVDC intertie," *Transactions on Power Apparatus and Systems, vol. 95(2), pp. 536-541*, 1976.

[4] S. Boersma, X. Bombois, L. Vanfretti, V. Peric, J. C. Gonzalez-Torres, R. Segur, and A. Benchaib, "Enhanced power system damping estimation via optimal probing signal design," *European Conference on Power Electronics and Applications*, 2020.

[5] D. N. Kosterev, C. W. Taylor, and W. A. Mittelstadt, "Model validation for the August 10, 1996 WSCC system outage," *Trans. Power Syst, vol. 14(3), pp. 967-979*, 1999.

[6] K. Uhlen, L. Vanfretti, M. M. de Oliveira, A. B. Leirbukt, V. H. Aarstrand, and J. O. Gjerde, "Wide-area power oscillation damper implementation and testing in the Norwegian transmission network," *Power and Energy Society General Meeting*, 2012.

[7] D. Schoenwald, "Wide area damping control: proof of concept," tech. rep., Sandia National Laboratories, 2014.

[8] B. Trudnowski, D. Pierre, F. Wilches-Bernal, D. Schoenwald, R. Elliot, J. Neely, R. Byrne, and D. Kosterev, "Initial closed-loop testing results for the pacific DC intertie wide area damping controller," *Power Energy Society General Meeting*, 2017.

[9] S. M. Badran and M. A. Choudhry, "Design of modulation controllers for AC/DC power systems," *Trans. Power Syst, vol. 8(4), pp. 1490-1496*, 1993.

[10] R. Eriksson and L. Söder, "Coordinated control design of multiple HVDC links based on model identification," *Computers & Mathematics with Applications, vol.60(4), pp. 944-953*, 2010.

[11] R. Preece, J. V. Milanović, A. M. Almutairi, and O. Marjanovic, "Probabilistic evaluation of damping controller in networks with multiple VSC-HVDC lines," *Trans. Power Syst, vol. 28(1), pp. 367-376*, 2013.

[12] J. C. Gonzalez-Torres, V. Costan, G. Damm, A. Benchaib, and F. Lamnabhi-Lagarrigue, "Dynamic control of embedded HVDC to contribute to transient stability enhancement," *International Council on Large Electric Systems*, 2020.

[13] E. S. Subcommittee, "IEEE Tutorial course power system stabilization via excitation control," tech. rep., IEEE Power Engineering Society Life Long Learning Committee, 2007.

[14] K. Tanaka and H. O. Wang, *Fuzzy Control Systems Design and Analysis*. John Wiley & Sons, Inc., 2001.

[15] M. Chilali and P. M. Gahinet, "Hinf design with pole placement constraints: an LMI approach," *Transactions on Automatic Control, vol. 41(3), pp. 358-367*, 1996.

[16] T. Söderström and P. Stoica, *System identification*. Prentice Hall, 1989.

[17] L. Ljung, *System identification: theory for the user*. Prentice Hall, 1999.

[18] M. Baudette, M. Castro, T. Rabuzin, J. Lavenius, T. Bogodorova, and L. Vanfretti, "OpenIPSL: Open-Instance Power System Library - Update 1.5 to "iTesla Power Systems Library (iPSL): A Modelica library for phasor time-domain simulations"," *SoftwareX, vol. 7, pp. 2352-7110*, 2018.

[19] M. Klein, G. J. Rogers, and P. Kundur, "A fundamental study of inter-area oscillations in power systems," *Trans. Power Syst, vol. 6(3), pp. 914-921*, 1991.

[20] B. J. Pierre, F. Wilches-Bernal, D. A. Schoenwald, R. T. Elliott, J. C. Neely, R. H. Byrne, and D. J. Trudnowski, "Open-loop testing results for the pacific DC intertie wide area damping controller," *Manchester PowerTech*, 2017.

[21] M. Baur, M. Otter, and B. Thiele, "Modelica Libraries for Linear Control Systems," *Proceedings of the 7th International Modelica Conference*, 2009.

[22] Y. Chompoobutrgool and L. Vanfretti, "Using PMU signals from dominant paths in wide-area damping control," *Sustainable Energy, Grids and Network, vol. 4, pp. 16-28*, 2015.

[23] K. J. Åström and R. M. Murray, *Feedback Systems*. Princeton University Press, 2009.